Journal of Applied Mathematics and Physics (ZAMP)
Vol. 37, July 1986

0044-2275/86/004608-16 $ 4.70/0

Subharmonic and asymmetric convection rolls

By F. H. Busse, Universität von Bayreuth, West-Germany, and Institute of Geophysics and Planetary Physics, University of California at Los Angeles and by A. C. Or, Dept. of Earth and Space Sciences, University of California at Los Angeles, USA

1. Introduction

Convection rolls in a horizontal fluid layer heated from below represent one of the most intensively studied solutions of the basic equations of fluid dynamics. Analytical solutions valid at small amplitudes of motion as well as numerical solutions for large Rayleigh numbers have been obtained in numerous publications. The common property of these solutions is the spatial periodicity described by the wavenumber α and the reflection symmetry for the vertical velocity w,

$$w(x, z) = -w\left(\frac{\pi}{\alpha} - x, -z\right) \tag{1.1}$$

provided the boundary conditions at $z = \pm \frac{1}{2}$ are symmetric and no asymmetries with respect to the midplane $z = 0$ are introduced by the fluid properties. Here and in the following dimensionless variables are used based on the layer thickness d as length scale, d^2/κ as time scale, where κ is the thermal diffusivity, and $T_2 - T_1$ as scale of the temperature, where T_2 and T_1 are the temperatures of the lower and upper boundaries, respectively.

A class of two-dimensional solutions which do not exhibit the symmetry (1.1) has been derived by Segel [8] and by Knobloch and Guckenheimer [5] in the case of stress-free boundaries. This class of solutions corresponds closely to the subharmonic solutions which have been found [1, 3, 6] in the Taylor vortex problem. We shall call this type of solution which describes the transition from a double roll to a single roll the transition solution. It possesses vertical planes of symmetry such that

$$w(x - x_0, z) = w(x_0 - x, z) \tag{1.2}$$

is satisfied for selected values of x_0.

In this paper we derive a new class of solutions which does no longer possess either of symmetries (1.1) or (1.2). The new kind of solution, called the mean

component solution, exhibits the same bifurcation properties in lowest order as the transition solution. Thus it is found that it is usually unstable except possibly for low Prandtl numbers. But this new type of solution is of interest from a more general physical point of view. First, there are unusual properties associated with this solution as, for example, a mean vorticity component. Secondly, because the new solution appears in two dual versions, it is likely to persist under more complex physical conditions for which one or the other version may be stable for a wide range of the parameter space.

The mathematical analysis presented in this paper is divided into two parts. First a general analytical theory of mixed solutions will be described in Sect. 2. The transition solutions of [5, 8] and the mean component solutions evaluated explicitly in this paper are but special examples of the general class of mixed solutions that is derived in Sect. 2. Properties of higher order are considered in Sect. 3 and the stability properties of the solutions are outlined in Sect. 4. The second part of the paper starts in Sect. 5 and describes a numerical analysis based on a Galerkin scheme for both the mean component and the transition solution. The paper ends with some concluding remarks in which related previous work is discussed.

2. Small amplitude analysis

For the description of two-dimensional convection it is convenient to introduce a streamfunction, $w = \partial_x \psi$, $u = -\partial_z \psi$, where u is the velocity component in the horizontal x-direction and ∂_z denotes the partial derivative with respect to z. The nondimensional equation of motion for ψ and the heat equation for the deviation θ from the temperature distribution of the static state can be written in the form

$$\nabla^4 \psi + R\,\partial_x \theta = P^{-1}\left(\frac{\partial}{\partial t} - \partial_z \psi\,\partial_x + \partial_x \psi\,\partial_z\right)\nabla^2 \psi \tag{2.1 a}$$

$$\nabla^2 \theta + \partial_x \psi = \left(\frac{\partial}{\partial t} - \partial_z \psi\,\partial_x + \partial_x \psi\,\partial_z\right)\theta \tag{2.1 b}$$

where P is the Prandtl number. The boundary conditions are

$$\psi = \partial_{zz}^2 \psi = \theta = 0 \quad \text{at} \quad z = \pm \tfrac{1}{2}. \tag{2.2}$$

Without introducing a formal expansion parameter we seek steady solutions of the form

$$\begin{aligned} \psi &= \psi_0 + \psi_1 + \psi_2 + \cdots \\ \theta &= \theta_0 + \theta_1 + \theta_2 + \cdots \\ R &= R_0 + R_1 + R_2 + \cdots \end{aligned} \tag{2.3}$$

where ψ_0, θ_0 and R_1 are linear in the amplitude of convection; ψ_1, θ_1 and R_2 are quadratic and so on.

The linearized version of Eq. (2.1) for which the right hand sides vanish admits the solutions

$$\psi_0 = [A \sin \alpha x + B \sin(\beta x + \chi)] \sin \pi (z + \tfrac{1}{2}) \equiv A \psi^{(1)} + B \psi^{(2)} \tag{2.4}$$

$$\theta_0 = R_0^{-1} [A (\pi^2 + \alpha^2)^2 \alpha^{-1} \cos \alpha x + B (\pi^2 + \beta^2)^2 \beta^{-1} \cos(\beta x + \chi)] \sin \pi (z + \tfrac{1}{2}) \equiv A \theta^{(1)} + B \theta^{(2)} \tag{2.5}$$

provided that the wavenumbers α and β satisfy the condition

$$R_0 \equiv (\pi^2 + \hat{\alpha}^2)^3 \hat{\alpha}^{-2} = (\pi^2 + \hat{\beta}^2)^3 \hat{\beta}^{-2}. \tag{2.6}$$

For example in the case $\hat{\beta} = 2\hat{\alpha}$ this condition yields a cubic equation for $(\hat{\alpha}/\pi)^2$,

$$20 (\hat{\alpha}/\pi)^6 + 12 (\hat{\alpha}/\pi)^4 = 1 \tag{2.7}$$

the positive root of which gives the approximate value

$$\hat{\alpha} = 1.5501534. \tag{2.8a}$$

The corresponding value of R_0 is given by

$$\hat{R} = 769.234 \tag{2.8b}$$

and exceeds the critical value obtained for $\alpha_c = \pi/\sqrt{2}$ by about 17%. But in general α and β do not have to be commensurate and R_0 may approach the critical value closely.

In order to determine the dependence of the amplitudes A and B on the Rayleigh number, the higher orders of Eqs. (2.1) must be considered. We obtain the solvability conditions for the inhomogeneous linear equations for ψ_1, θ_1 by multiplying (2.1a) by $\psi^{(n)}$ and (2.1b) by $-R_0 \theta^{(n)}$ adding the equations and averaging them over the fluid layer for $n = 1, 2$. Here $\psi^{(n)}$, $\theta^{(n)}$ with $n = 1, 2$ represent the functions defined in expressions (2.4) and (2.5). For reasons of symmetry the three solvability conditions are trivially satisfied with $R_1 = 0$. The solution for ψ_1, θ_1 is given by

$$\begin{aligned}\psi_1 = {} & \tfrac{1}{4} A B \pi \sin 2\pi (z + \tfrac{1}{2}) (\beta^2 - \alpha^2) \\ & \cdot \{\sin[(\alpha + \beta) x + \chi] D_+ [a_2^2/\beta - a_1^2/\alpha + P^{-1} (\beta - \alpha) b_+] \\ & - \sin[(\beta - \alpha) x + \chi] D_- [a_2^2/\beta + a_1^2/\alpha + P^{-1} (\beta + \alpha) b_-]\}\end{aligned} \tag{2.9a}$$

$$\begin{aligned}\theta_1 = {} & -\sin 2\pi \left(z + \frac{1}{2}\right) \frac{1}{8\pi R_0} (A^2 a_1^2 + B^2 a_2^2) + \frac{1}{4} A B \pi \sin 2\pi \left(z + \frac{1}{2}\right) \\ & \cdot \{\cos[(\beta + \alpha) x + \chi] D_+ [b_+^2 (\beta - \alpha) R_0^{-1} (a_2^2/\beta - a_1^2/\alpha) + P^{-1} (\beta^2 - \alpha^2)^2] \\ & - \cos[(\beta - \alpha) x + \chi] D_- [b_-^2 (\beta + \alpha) R_0^{-1} [a_2^2/\beta + a_1^2/\alpha] \\ & + P^{-1} (\beta^2 - \alpha^2)^2]\}\end{aligned} \tag{2.9b}$$

where the following definitions have been used

$$a_1 \equiv \pi^2 + \alpha^2, \quad a_2 \equiv \pi^2 + \beta^2, \quad b_+ \equiv 4\pi^2 + (\beta + \alpha)^2,$$
$$b_- \equiv 4\pi^2 + (\beta - \alpha)^2, \quad D_+ \equiv [b_+^3 - R_0(\beta + \alpha)^2]^{-1},$$
$$D_- \equiv [b_-^3 - R_0(\beta - \alpha)^2]^{-1}. \tag{2.9c}$$

After inserting the expressions for ψ_1, θ_1 on the right hand side of Eqs. (2.1) the solvability conditions for the equations for ψ_2, θ_2 can be obtained,

$$R_2 \langle \psi^{(n)} \partial_x \theta_0 \rangle$$
$$= - R_0 \langle \theta^{(n)}, (\partial_x \psi_1 \partial_z - \partial_z \psi_1 \partial_x)\theta_0 + (\partial_x \psi_0 \partial_z - \partial_z \psi_0 \partial_x)\theta_1 \rangle$$
$$+ \langle \psi^{(n)}, (\partial_x \psi_1 \partial_z - \partial_z \psi_1 \partial_x)\nabla^2 \psi_0 + (\partial_x \psi_0 \partial_z - \partial_z \psi_0 \partial_x)\nabla^2 \psi_1 \rangle. \tag{2.10}$$

The evaluation of this equation for $n = 1, 2$ yields two equations for A and B,

$$\left\{R - \hat{R} - \left.\frac{\partial R_0}{\partial \alpha}\right|_{\hat{\alpha}} (\alpha - \hat{\alpha}) - f_0 A^2 - [g_0 + f_1(P)] B^2\right\} A = 0 \tag{2.11a}$$

$$\left\{R - \hat{R} - \left.\frac{\partial R_0}{\partial \alpha}\right|_{\hat{\beta}} (\beta - \hat{\beta}) - g_0 B^2 - [f_0 + g_1(P)] A^2\right\} B = 0. \tag{2.11b}$$

In writing these equations we have neglected terms of higher than third power in the amplitude and we have allowed for small differences between α, β and $\hat{\alpha}$, $\hat{\beta}$, where the latter symbols refer to the specific values for which relationship (2.6) holds with $\hat{\beta} > \hat{\alpha}$. The constants f_0 and g_0 are given by

$$f_0 = \tfrac{1}{8}(\pi^2 + \hat{\alpha}^2)^2, \quad g_0 = \tfrac{1}{8}(\pi^2 + \hat{\beta}^2)^2$$

while the functions $f_1(P)$ and $g_1(P)$ are given in the Appendix. In the special case $\hat{\beta} = 2\hat{\alpha}$, f_1 and g_1 are of the order 50 and 20, respectively, at large Prandtl numbers and grow like $-P^{-2}$ and P^{-2}, respectively, for small Prandtl numbers. $f_1(P)$ changes sign at $P = P \cong 0.397$, while $g_1(P)$ increases monotonically with P^{-1}.

Besides the normal convection solutions of (2.11),

$$A^2 = (R - R_0)/f_0, \quad B = 0 \quad \text{and} \quad B^2 = (R - R_0)/g_0, \quad A = 0 \tag{2.12a, b}$$

there exists a third solution of Eqs. (2.11),

$$A^2 = N^{-1}\left\{(R - \hat{R}) f_1 + (\alpha - \hat{\alpha}) \left.\frac{\partial R_0}{\partial \alpha}\right|_{\hat{\alpha}} g_0 - (\beta - \hat{\beta}) \left.\frac{\partial R_0}{\partial \alpha}\right|_{\hat{\beta}} (g_0 + f_1)\right\} \tag{2.13a}$$

$$B^2 = N^{-1}\left\{(R - \hat{R}) g_1 + (\beta - \hat{\beta}) \left.\frac{\partial R_0}{\partial \alpha}\right|_{\hat{\beta}} f_0 - (\alpha - \hat{\alpha}) \left.\frac{\partial R_0}{\partial \alpha}\right|_{\hat{\alpha}} (f_0 + g_1)\right\} \tag{2.13b}$$

where the function $N(P)$ is defined by

$$N(P) \equiv g_0 g_1 + f_0 f_1 + f_1 g_1 . \tag{2.14}$$

Periodic solutions of the form (2.13) with $\beta = r\alpha$, where r is a rational number, exist in the interval

$$S_1 (R - \hat{R}) \gtrless \hat{\alpha} - \alpha \gtrless S_2 (R - \hat{R}) \quad \text{for} \quad \begin{matrix} N > 0 \\ N < 0 \end{matrix} \quad \text{and} \quad P \geqq P_d \tag{2.15}$$

where the functions S_1 and S_2 are given by

$$S_1 \equiv g_1 \left[r \left. \frac{\partial R_0}{\partial \alpha} \right|_{r\hat{\alpha}} f_0 - \left. \frac{\partial R_0}{\partial \alpha} \right|_{\hat{\alpha}} (f_0 + g_1) \right]^{-1} \tag{2.16a}$$

$$S_2 \equiv f_1 \left[\left. \frac{\partial R_0}{\partial \alpha} \right|_{\hat{\alpha}} g_0 - r \left. \frac{\partial R_0}{\partial \alpha} \right|_{r\hat{\alpha}} (g_0 + f_1) \right]^{-1} . \tag{2.16b}$$

They satisfy the relationship

$$S_1^{-1} - S_2^{-1} = \left[r \left. \frac{\partial R_0}{\partial \alpha} \right|_{r\hat{\alpha}} - \left. \frac{\partial R}{\partial \alpha} \right|_{\hat{\alpha}} \right] N / f_1 g_1 . \tag{2.17}$$

In the special case $r = 2$ the functions S_1 and S_2 are plotted in Fig. 1 as a function of the Prandtl number. S_2 is negative for $P > P_z \cong 0.397$ and solution (2.13) exists for $\alpha > \hat{\alpha}$ in this regime. The interval (2.15) decreases as S_2 approaches S_1 for decreasing Prandtl number and vanishes at $P \cong 0.296$ where S_1 equals S_2 and $N(P)$ changes sign. For $P < 0.296$ the interval of existence rapidly increases as S_2 tends to infinity. This divergence of S_2 occurs at $P = P_d \cong 0.234$ and

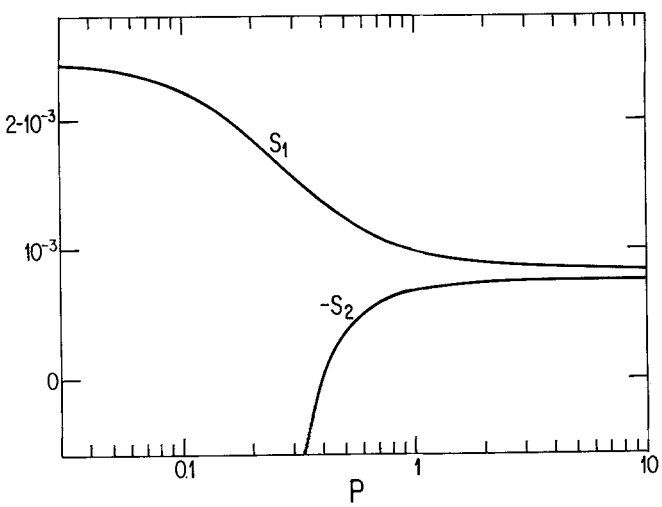

Figure 1
S_1 and $-S_2$ as functions of the Prandtl number P.

indicates that the interval of existence is no longer bounded towards small values of α as P decreases even further,

$$\alpha < \hat{\alpha} - S_1 (R - \hat{R}) \quad \text{for} \quad P < P_d. \tag{2.18}$$

It must be remembered, of course, that the small amplitude analysis requires $|\hat{\alpha} - \alpha| \ll 1$ and the lower bound for α must be obtained from different considerations. We shall return to this point in later sections of this paper.

The solution (2.13) bifurcates from solution (2.12a) on the left side of the interval (2.15) and joins solution (2.12b) on the right hand side of the interval (2.15). In the special case $\chi = 0, r = 2$ solution (2.13) thus describes the transition from a double roll pair within the region $0 \leqq x \leqq 2\pi/\alpha$ at the right side of the interval (2.15) to a single roll pair at the left side of (2.15). We shall call this solution the transition solution for this reason.

In the case of solution (2.12) a change of the sign of A and B does not lead to a new solution; it just corresponds to a horizontal translation by half a wavelength. If, however, in the case of solution (2.13) the signs of B or A or of both are changed, then new solutions are obtained. The number of solutions is reduced only in special cases. For example in the case $\beta = 2\alpha$, a new solution is obtained only by a change of sign of B since a change of sign of A corresponds to a translation by π/α. These two solutions exhibit the reflection symmetry (1.1) with respect to each other,

$$w(x, z) = - w^* \left(\frac{\pi}{\alpha} - x, - z \right) \tag{2.19}$$

where the asterisk* refers to the solution obtained by a change of sign B. This property which holds for all orders of the expansion (2.3) depends, of course, on the basic symmetry of the convection layer that we are considering. Once asymmetries such as a temperature dependent viscosity appear, the symmetry (2.19) disappears and the two conjugate solutions will differ in their gross physical properties such as the convective heat transport.

As we have shown in Sect. 2 the analysis for the general form (2.4) of the solution is essentially identical up to second order terms with the analyses of Segel [8] and of Knobloch and Guckenheimer [5] in the special case $\chi = 0$, $\beta = (k + 1)\alpha/k$. This property continues to hold for the stability analysis which is outlined in Sect. 4.

3. Higher order properties

The relationships that have been discussed so far hold independently of the phase angle χ. In the case of periodic solutions however the phase angle may enter explicitly the solvability conditions of higher order. We consider this problem in this section by focussing the attention on the special case $\beta = 2\alpha$.

In contrast to solutions (2.12) a finite mean component $\bar{\psi}$ must be expected for solutions of the form (2.13). By taking the x-average of the equations of motion we obtain as equation for $\bar{\psi}$

$$\partial_{zzz}^3 \bar{\psi} = P^{-1} \partial_z (\overline{\partial_z \psi \partial_x \psi}) \tag{3.1}$$

where the bar indicates the average over the x-dependence. Integration of (3.1) yields

$$\partial_{zz}^2 \bar{\psi} = P^{-1} \overline{\partial_z \psi \partial_x \psi} \tag{3.2}$$

The constant of integration vanishes because of the assumption of stress-free boundaries. A non-vanishing contribution to $\bar{\psi}$ can be obtained first in third order,

$$\partial_{zz}^2 \bar{\psi}_2 = P^{-1} (\overline{\partial_z \psi_0 \partial_z \psi_1} + \overline{\partial_x \psi_1 \partial_z \psi_0}). \tag{3.3}$$

The evaluation and integration of this relationship yields

$$\bar{\psi}_2 = - P^{-1} A^2 B \sin\chi \frac{\alpha^2}{144} \cdot \left[36 \sin \pi\left(z + \frac{1}{2}\right) - \sin 3\pi\left(z + \frac{1}{2}\right)\right](a_2 P^{-1} 9\alpha^2 + 3a_2^2/2 + 3a_1^2) D_- . \tag{3.4}$$

In the case of the transition solution, $\chi = 0$, the mean component of ψ vanishes. This property must be expected on the basis of the symmetry property (1.2). For finite χ modulo π this symmetry no longer holds and the two dual solutions corresponding to the two signs of B exhibit a mean component $\bar{\psi}$. The nonlinear interactions which give rise to a finite $\bar{\psi}_2$ may also lead to restrictive solvability conditions in higher order unless χ is an integer multiple of $\pi/2$. This is suggested by the numerical analysis in which solutions within the interval $0 < \chi < \pi/2$ have not been obtained. The solution for $\chi = \pi/2$ which maximises the mean component $\bar{\psi}_2$ will be called the mean component solution in the following.

Although a finite $\bar{\psi}$ describes a mean flow in the sense of the averaged velocity field, it does not imply that fluid particles move arbitrarily long distances given enough time. The streamline pictures for the transition solution and the mean component solution shown in Figs. 4 and 5 show that both solutions correspond to closed streamlines. But anticlockwise vorticity dominates in Fig. 5 corresponding to a positive value of B in expression (3.4) with $\sin\chi = 1$. The figures also indicate the property that the mean component solution does not possess a vertical plane of symmetry while the transition solution obeys the relationships $\psi(x) = -\psi(-x)$ and $\psi\left(x + \frac{\pi}{\alpha}\right) = -\psi\left(\frac{\pi}{\alpha} - x\right)$.

4. Stability analysis

The simultaneous existence of solutions of the forms (2.12), (2.13) for given values of R, α, β suggests that most of them are unstable and only one is possibly stable. A restricted stability analysis can be accomplished readily by an extension of the analysis of Sect. 2.

After superimposing infinitesimal disturbances onto the steady solutions,

$$A + \tilde{A}\exp(\sigma t), \quad B + \tilde{B}\exp(\sigma t)$$

we obtain the following equations for $\tilde{A}$ and $\tilde{B}$ in analogy to Eqs. (2.11)

$$\sigma M_1 \tilde{A} = [(R - R_1) - 3 f_0 A^2 - (g_0 + f_1) B^2]\tilde{A} - 2(g_0 + f_1) B A \tilde{B} \quad (4.1\,a)$$

$$\sigma M_2 \tilde{B} = [(R - R_2) - 3 g_0 B^2 - (f_0 + g_1) A^2]\tilde{B} - 2(f_0 + g_1) A B \tilde{A} \quad (4.1\,b)$$

where the definitions

$$M_1 \equiv \hat{\alpha}^2(1 + P^{-1}), \quad M_2 \equiv \hat{\beta}^2(1 + P^{-1})$$

$$R_1 = \hat{R} + (\alpha - \hat{\alpha})\left.\frac{\partial R_0}{\partial \alpha}\right|_{\hat{\alpha}}, \quad R_2 = \hat{R} + (\beta - \hat{\beta})\left.\frac{\partial R_0}{\partial \alpha}\right|_{\hat{\beta}}$$

have been introduced. The condition that the determinant of the coefficient matrix for the system (4.1) vanishes yields a quadratic equation for the growth-rate σ. In the case of the three solutions (2.12a), (2.12b), (2.13) the conditions for stabilitiy assume the following forms

$$-f_0(R_2 - R_1) - g_1(R - R_1) < 0 \quad \text{for} \quad A^2 = (R - R_1)/f_0, \quad B = 0 \quad (4.2\,a)$$

$$-g_0(R_1 - R_2) - f_1(R - R_2) < 0 \quad \text{for} \quad B^2 = (R - R_2)/g_0, \quad A = 0 \quad (4.2\,b)$$

$$N(P) < 0 \quad \text{for the mixed solutions.} \quad (4.2\,c)$$

Since the expressions on the left hand side of the inequalities (4.2a) and (4.2b) are identical to the wavy brackets of expressions (2.13b) and (2.13a) except for the sign, the expected connection between instability and the bifurcation of a new solution is evident.

We now return to the special case $\beta = 2\alpha$ which we use as an example. For $P > P_z$ the bifurcation is relatively simple. The diagrams for $\alpha > \hat{\alpha}$ and $\alpha < \hat{\alpha}$ are shown in Fig. 2. Because $N(P)$ is positive the mixed solutions are always

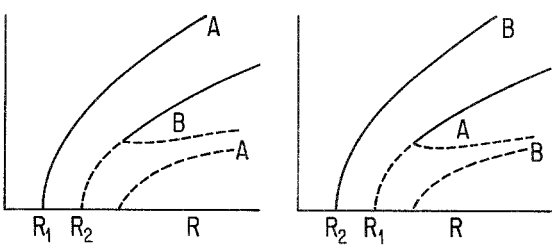

Figure 2
Bifurcation diagrams in the case $P > P_z$ for $\alpha > \hat{\alpha}$ (left) and for $\alpha < \hat{\alpha}$ (right). Dashed lines correspond to unstable branches. The mixed solutions (2.13) are unstable everywhere.

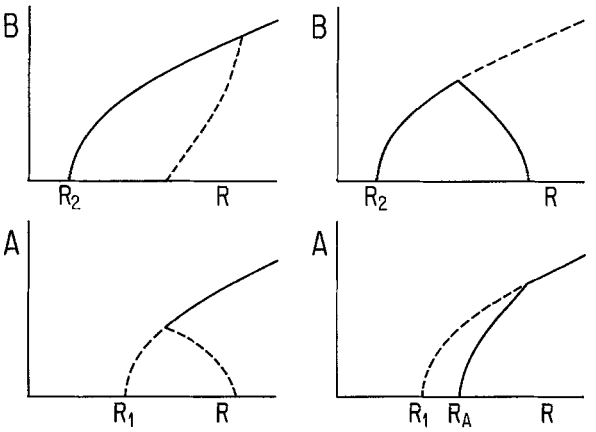

Figure 3
Bifurcation diagrams for $P < P_z$ in case $N > 0$ (left) and in the case $N < 0$ (right). Dashed lines indicate unstable branches. The bifurcation point R_A moves to the left of R_1 as the Prandtl number decreases below 0.28.

unstable. More interesting features appear when P is less than P_z. Since the existence of the mixed solutions is restricted in this case to the region $\alpha < \hat{\alpha}$ or $R_2 < R_1$ the interval (2.15) also defines a finite interval of existence in terms of the Rayleigh number for a given value of α. Fig. 3a describes the bifurcation diagram for $N > 0$; Fig. 3b indicates the changes that occur when N changes sign. In between the domain of existence of the mixed solution vanishes as N approaches zero. The bifurcation point R_A actually drops below R_1 as f_1 decreases below $-g_0$ which happens at $P \cong 0.280$; for even smaller Prandtl numbers R_A approaches R_2. We thus find that a solution with a finite value of A exists below the Rayleigh number for onset of convection with the wavenumber α. For a general discussion of the bifurcation problems described by equations of the form (2.13) we refer to Golubitsky and Schaeffer [4] where the diagrams of Figs. 2 and 3 are included as special cases.

5. Numerical analysis

The numerical analysis complements the analytical theory in that it yields results in the high Rayleigh number domain where the expansion (2.3) looses validity. On the other hand it becomes more difficult to extract the parameter dependence from the computed solutions which is directly available from the explicit expressions (2.13). The numerical method which resembles the analytical treatment most closely is the Galerkin method in which the dependent variables are represented by the same set of functions which also appear in the perturbation approach,

$$\psi = \sum_{l,n} (\hat{a}_{ln} \cos n\alpha x + \check{a}_{ln} \sin n\alpha x) \sin l\pi(z + \tfrac{1}{2}) \tag{5.1a}$$

$$\theta = \sum_{l,n} (\hat{b}_{ln} \cos n\alpha x + \check{b}_{ln} \sin n\alpha x) \sin l\pi(z + \tfrac{1}{2}). \tag{5.1b}$$

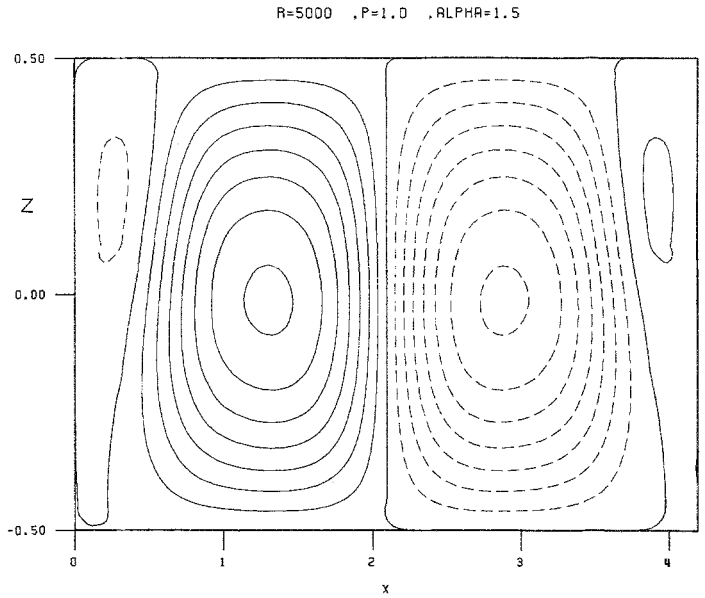

Figure 4
Streamlines ψ = const of the transition solution for $R = 5000$, $P = 1$, $\alpha = 1.5$.

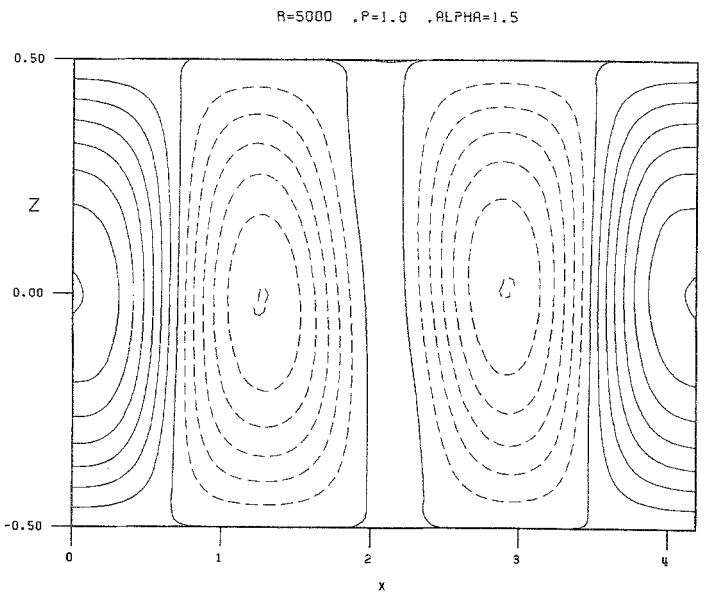

Figure 5
Streamlines $\hat{\psi}$ = const of the mean component solution for $R = 5000$, $P = 1$, $\alpha = 1.5$.

After inserting this representation into Eqs. (2.1), multiplying them by $\cos m\alpha x \sin k\pi(z+\frac{1}{2})$ and $\sin m\alpha x \sin k\pi(z+\frac{1}{2})$ and averaging them over the fluid layer, we obtain a system of nonlinear algebraic equations for the unknowns $\hat{a}_{km}$, $\check{a}_{km}$, $\hat{b}_{km}$, $\check{b}_{km}$. In order to reduce the number of terms we have restricted the attention to periodic solutions and specifically to those with $\beta = 2\alpha$ among them. The simplest solution corresponds to solution (2.12a) and is characterized by the symmetry properties

$$\begin{aligned} &\hat{a}_{ln} = 0 \quad \text{for all} \quad l, n, \quad \check{a}_{ln} = 0 \quad \text{for} \quad l+n = \text{odd} \\ &\hat{b}_{ln} = 0 \quad \text{for} \quad l+n = \text{odd}, \quad \check{b}_{ln} = 0 \quad \text{for all} \quad l, n. \end{aligned} \tag{5.2}$$

An infinite number of solutions of the form (5.1) can be obtained from solution (5.2) by a translation. Since we are only interested in physically different solutions we shall ignore this degeneracy of the problem. The convection field described by a solution of the form (5.2) can also be described by a different set of coefficients when α is replaced by $\tilde{\alpha} = \alpha/m$ in representation (5.1) where m is an integer. It is thus important to distinguish between these sets of mathematical solutions which describe the same physical solution and those which describe a physically different solution.

The transition solution and the mean component solution represent novel solutions which are physically distinguished from solutions of the form (5.2). The transition solution in its simplest form is characterized by

$$\begin{aligned} &\hat{a}_{ln} = \check{b}_{ln} = 0 \quad \text{for all} \quad l, n \\ &\check{a}_{ln} = \pm\, \check{a}^*_{ln} \quad \text{and} \quad \hat{b}_{ln} = \pm\, \hat{b}^*_{ln} \quad \text{for} \quad l+n = \begin{cases} \text{even} \\ \text{odd} \end{cases} \end{aligned} \tag{5.3}$$

where the symbol * refers again to the conjugate solution. The mean component solution is characterized by

$$\begin{aligned} &\hat{a}_{ln} = \check{b}_{ln} = 0 \quad \text{for} \quad l = \text{even}, \\ &\hat{a}_{ln} = \pm\, \hat{a}^*_{ln} \quad \text{and} \quad \check{b}_{ln} = \pm\, \check{b}^*_{ln} \quad \text{for} \quad n = \begin{cases} \text{odd} \\ \text{even} \end{cases} \\ &\check{a}_{ln} = \hat{b}_{ln} = 0 \quad \text{for} \quad l = \text{odd}, \\ &\check{a}_{ln} = \pm\, \check{a}^*_{ln} \quad \text{and} \quad \hat{b}_{ln} = -\, \hat{b}^*_{ln} \quad n = \begin{cases} \text{even} \\ \text{odd} \end{cases} \end{aligned} \tag{5.4}$$

Other representations can be obtained, of course, by shifting the solution by a quarter of a wavelength, as in the case of expression (2.4) for $\chi = \frac{\pi}{2}$. The transition solution and the mean component solution continue to bifurcate at the same value α_2. But away from the bifurcation point their amplitudes differ in contrast to the conclusion based on the solvability condition in the third order. Figure 6 shows the dependence of the dominant coefficients on α.

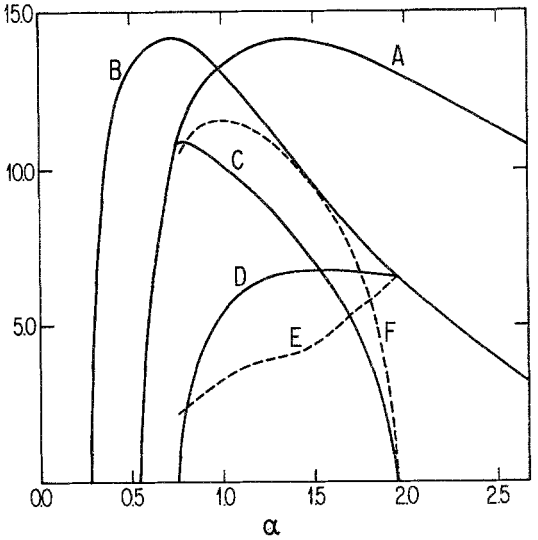

Figure 6
Bifurcation diagram as a function of α for $R = 3500$, $P = 1$. Curves A and B describe the coefficients $\hat{a}_{11}$ and $\hat{a}_{12}$ corresponding to the symmetric solutions (2.12). The lines C and D give the coefficients $\hat{a}_{11}$ and $\hat{a}_{12}$ for the mean component solution, while the dashed lines E and F describe $\check{a}_{11}$ and $\check{a}_{12}$ for the transition solution. The dashed lines are expected to join the solid lines at a point of bifurcation on the left side. But the numerical solution ceased to converge in the neighborhood of the left bifurcation point.

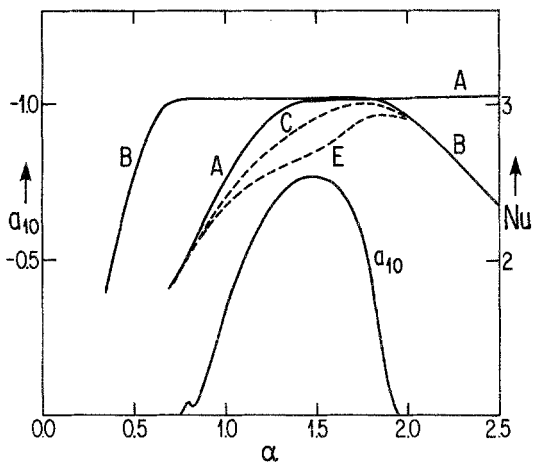

Figure 7
The coefficient $\hat{a}_{10}$ of the mean component solution (left scale) and the Nusselt numbers (right scale) for the symmetric solutions (A, B), for the mean component solution (C), and for the transition solution (E). All curves have been computed for $R = 3500$, $P = 1.0$.

Problems of numerical convergence have prevented us to complete the curves for the transition solution near the point of bifurcation $\alpha = \alpha_1$. Apparently the solution overshoots slightly into the region $\alpha < \alpha_1$ before reaching the bifurcation point at $\alpha = \alpha_1$. Armbruster [private Communication, 1986] has shown that higher order terms cause a difference between the bifurcation points α_1 for the transition solution and the mean component solution. In the same analysis he also shows that the latter solution is stable while the former becomes unstable for $N < 0$.

6. Concluding remarks

The phenomenon of mixed solutions arising from the coincidence of the eigenvalues of two linear eigenmodes has been studied in the case of the Taylor

vortex instability [1, 3, 5, 6]. But the asymmetry of the external conditions in that case and the use of rigid boundaries have prohibited an entirely analytical solution, even when the limit of small amplitudes was adopted [1]. As has been noted in [4] the transition solution for a stress-free convection layer corresponds closely to the mixed solutions studied in the Taylor vortex case. The analogon of the mean flow solution has not been studied in the Taylor vortex case because a symmetry assumption has usually been made which corresponds to assumption (1.2) in the case of convection. The general axissymmetric Taylor-Couette problem is equivalent, of course, to two-dimensional convection in a layer with asymmetries. Only in the limit of a small gap and nearly corotating cylinders does the Taylor-Couette problem coincide with the problem of two-dimensional convection considered in this paper after stress-free boundaries have been replaced by rigid ones. The transition solution and its conjugate solution begin to differ in their physical properties such as the heat transport as soon as asymmetric properties are introduced in the convection layer. Moreover, they can no longer be distinguished from the "symmetric" solution (2.12a) by symmetry properties. The comparison with the results of [6, 7] indicates that the bifurcation point where these three solutions come together disappears just as a pitchfork bifurcation disintegrates into two separate branches when imperfections are introduced. On the other hand, the bifurcation point where the two transition solutions join the solution (2.12b) separates into two bifurcation points. In fact, it is appropriate to distinguish two solutions of the type (2.12b) which differ by a translation of $\pi/2\alpha$ in the x-direction. The qualitative change introduced by an asymmetric property in the bifurcation diagram as a function of the wavenumber has been sketched in Fig. 8. It appears that the imperfect pitchfork bifurcation gives rise to the fold which is typically observed in the Taylor vortex case [6, 7].

The mean component solution has not been considered in the previous work since it does not possess the symmetry property (1.2). Undoubtedly it exists in the Taylor-Couette problem as well as in the problem of convection.

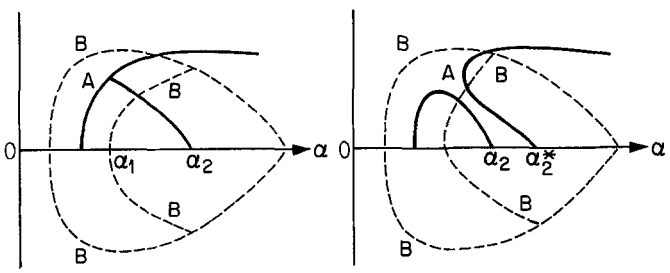

Figure 8
Qualitative sketch of bifurcating solutions. Dependence of A (solid lines) and B (dashed lines) on the wavenumber α is shown for a symmetric layer (left side, treated in this paper) and for a asymmetric layer (right side, Taylor vortex case). As asymmetries are introduced the pitchfork bifurcation at $\alpha = \alpha_1$ (left) disintegrates and the bifurcation point at $\alpha = \alpha_2$ splits into two separate bifurcation points at $\alpha = \alpha_2$, α_2^* (right).

Its most interesting property is the dominance of one sign of vorticity over the other. Situations where vortices of one sign are much stronger than those of the other sign have been observed as spiral vortices in the original experiments by Taylor [9]. Taylor remarks that they are likely to be induced by a basic large scale circulation in the apparatus. But it seems more likely that such a weak circulation may be important only indirectly in that it stabilizes one of the two mean component solutions of the problem.

An even simpler problem, where the phenomenon of mixed solution can be established is the problem of convection in a porous medium. However, porous medium convection lacks the advantage of an additional parameter, such as the Prandtl number. As has been demonstrated in [5, 8], this parameter influences the structure of the bifurcation diagram in an interesting way and raises the possibility of stable mixed solutions in an horizontally infinite layer. The limited stability analysis carried out so far does not prove general stability, of course. Even when two-dimensionality of convection is enforced by the application of a homogeneous magnetic field parallel to the axis of the convection rolls, there are still instabilities such as the Eckhaus instability that have been ignored so far. The latter instability is inhibited when convection in a finite box is considered as was actually done by Knobloch and Guckenheimer [5]. But the imposition of realistic rigid side walls instead of periodic ones is likely to change the properties of the mixed solution significantly, while only small quantitative differences must be expected when the stress-free horizontal boundaries are replaced by rigid ones.

The lower degree of symmetry of the mixed solutions does not offer any physical advantage in the case of the symmetric convection layer considered in [5] and in this paper. This situation may well change once layers with asymmetric properties are considered. Since the two pairs of conjugate solutions that correspond to the transition solution and to the mean component solution acquire different properties in that case, one of them may be especially adjusted to the external asymmetries and thus may become stable. An analogous, though physically different process occurs in the competition between hexagonal convection cells and convection rolls [2]. The search for suitable asymmetric properties thus seems promising.

Acknowledgement

The research reported in this paper has been supported in part by the Atmospheric Sciences Section of the U.S. National Science Foundation. The authors are grateful to Ms. R.-Q. Lin for help in the numerical computations, to Profs. E. Knobloch and E. A. Spiegel for pointing out papers [5] and [8], respectively, which the authors at first had overlooked, and to Dr. Rita Meyer-Spasche, Mr. H.-G. Paap and Mr. H. Riecke for numerous discussions.

Appendix

Using the definitions (2.9 c) with α, β, R_0 replaced by $\hat{\alpha}$, $\hat{\beta}$, $\hat{R}$, respectively, the function $f_1(P)$ and $g_1(P)$ can be written in the form

$$
\begin{aligned}
f_1(P) = \frac{\pi^2}{16}\Big\{ & D_+ [c_- + P^{-1}(\hat{\beta}-\hat{\alpha})b_+](\hat{\beta}-\hat{\alpha})(\hat{\beta}^2-\hat{\alpha}^2) \\
& \cdot [-a_2^2/\hat{\alpha}\hat{\beta} + P^{-1}\hat{R}(a_2-b_+)/a_1^2] \\
& + D_- [c_+ + P^{-1}(\hat{\beta}+\hat{\alpha})b_-](\beta+\alpha)(\hat{\beta}^2-\hat{\alpha}^2) \\
& \cdot [a_2^2/\hat{\alpha}\hat{\beta} + P^{-1}\hat{R}(a_2-b_-)/a_1^2] \\
& - D_+ [b_+^2(\hat{\beta}-\hat{\alpha})c_- + P^{-1}\hat{R}(\hat{\beta}^2-\hat{\alpha}^2)^2]\frac{\hat{\beta}-\hat{\alpha}}{\hat{\alpha}} \\
& + D_- [b_-^2(\hat{\beta}+\hat{\alpha})c_+ + P^{-1}\hat{R}(\hat{\beta}^2-\hat{\alpha}^2)^2]\frac{\hat{\beta}+\hat{\alpha}}{\hat{\alpha}}\Big\}
\end{aligned}
$$

$$
\begin{aligned}
g_1(P) = \frac{\pi^2}{16}\Big\{ & D_+ [c_- + P^{-1}(\hat{\beta}-\hat{\alpha})b_+](\hat{\beta}-\hat{\alpha})(\hat{\beta}^2-\hat{\alpha}^2) \\
& \cdot [a_1^2/\hat{\alpha}\hat{\beta} - P^{-1}\hat{R}(a_1-b_+)/a_2^2] \\
& + D_- [c_+ + P^{-1}(\hat{\beta}+\hat{\alpha})b_-](\hat{\beta}+\hat{\alpha})(\hat{\beta}^2-\hat{\alpha}^2) \\
& \cdot [-a_1^2/\hat{\alpha}\hat{\beta} - P^{-1}\hat{R}(a_1-b_-)/a_2^2] \\
& + D_+ [b_+^2(\hat{\beta}-\hat{\alpha})c_- + P^{-1}\hat{R}(\hat{\beta}^2-\hat{\alpha}^2)^2]\frac{\hat{\beta}-\hat{\alpha}}{\hat{\beta}} \\
& + D_- [b_-^2(\hat{\beta}+\hat{\alpha})c_+ + P^{-1}\hat{R}(\hat{\beta}^2-\hat{\alpha}^2)^2]\frac{\hat{\beta}+\hat{\alpha}}{\hat{\beta}}\Big\}
\end{aligned}
$$

where the following definition has been used,

$$c_\pm \equiv (\pi^2+\hat{\beta}^2)^2/\hat{\beta} \pm (\pi^2+\hat{\alpha}^2)^2/\hat{\alpha}\,.$$

The solvability condition (2.10) permits an additional contribution to $f_1(P)$ when the relationship $\hat{\beta} = 3\hat{\alpha}$ holds. But this contribution is vanishing because it is proportional to $3\hat{\alpha} - \hat{\beta}$.

References

[1] I. P. Andreichikov, *Branching of secondary modes in the flow between rotating cylinders.* Fluid Dynamics, Transl. from Izvestiya Akademii Nauk SSSR, Mekhanika Zhidkosti i Gaza, No. 1, 47–53 (1977).

[2] F. H. Busse, *The stability of finite amplitude convection and its relation to an extremum principle.* J. Fluid Mech. *30*, 625–649 (1967).

[3] G. Frank and R. Meyer-Spasche, *Computations of transitions in Taylor vortex flows.* J. Appl. Math. Phys. (ZAMP) *32,* 710–720 (1981).
[4] M. Golubitsky and D. G. Schaeffer, Chapt. 10, Sect. 4 of *Singularities and Groups in Bifurcation Theory, Vol. I.* Springer: New York, Berlin, Heidelberg, Tokyo 1985.
[5] E. Knobloch and J. Guckenheimer, *Convective transitions induced by a varying aspect ratio.* Phys. Rev. *A 27,* 408–417 (1983).
[6] R. Meyer-Spasche and H. B. Keller, *Some bifurcation diagrams for Taylor vortex flows.* Phys. Fluids *28,* 1248–1252 (1985).
[7] H. Riecke and H.-G. Paap, *Stability and Wavevector Restriction of Axisymmetric Taylor Vortex Flow.* Phys. Rev. A, *33,* 547–553 (1986).
[8] L. A. Segel, *The nonlinear interaction of two disturbances in the thermal convection problem.* J. Fluid Mech. *14,* 97–114 (1962).
[9] G. I. Taylor, *Stability of a viscous Liquid contained between Two Rotating Cylinders.* Trans. Roy. Soc. London *A223,* 289–343 (1923).

Summary

A new class of steady solutions is derived describing convection rolls which do not reflect the symmetry of the physical conditions of the convection layer. As does the class of mixed solutions considered by Segel (1962) and by Knobloch and Guckenheimer (1983) the new class arises from a wavelength doubling bifurcation. The new class is distinguished by a tilt of the convection rolls which gives rise to a finite mean horizontal component of vorticity. An analytic theory is derived for small amplitudes of motion in the case of stress-free boundaries. The theory is extended to higher amplitudes by numerical computations. The new solution shares with the solution of Segel, Knobloch and Guckenheimer the property that it is unstable for large Prandtl numbers P with respect to disturbances which tend to establish the wellknown symmetric solutions, but becomes stable with respect to these disturbances for Prandtl numbers $P \lessapprox 0.296$.

Zusammenfassung

Eine neue Klasse von Lösungen wird abgeleitet, welche Konvektionsrollen beschreibt, die nicht der Symmetrie der physikalischen Bedingungen der Schicht entsprechen. Ebenso wie die von Segel (1962) und von Knobloch und Guckenheimer (1983) abgeleitete Klasse von gemischten Lösungen geht die neue Klasse von Lösungen aus einer Verzweigung mit Wellenlängenverdopplung hervor. Die neue Klasse zeigt eine Schrägstellung der Rollen, die zu einer endlichen gemittelten horizontalen Komponente der Wirbelstärke führt. Eine analytische Theorie wird für den Fall kleiner Amplituden der Bewegung bei spannungsfreien Randbedingungen abgeleitet. Durch numerische Rechnungen wird die Theorie zu höheren Amplituden hin erweitert. Die neue Lösung hat mit der Lösung von Segel, Knobloch und Guckenheimer die Eigenschaft gemeinsam, daß sie instabil ist für große Prandtlzahlen P gegenüber Störungen, welche zu den bekannten symmetrischen Lösungen führen; für Prandtlzahlen $P \lessapprox 0.296$ ist sie aber stabil gegenüber diesen Störungen.

(Received: November 22, 1985; revised: March 5, 1986)